



Published in final edited form as:

Biochem Biophys Res Commun. 2020 November 05; 532(2): 244–250. doi:10.1016/j.bbrc.2020.08.026.

UDP-glucosyltransferase UGT84B1 regulates the levels of indole-3-acetic acid and phenylacetic acid in Arabidopsis

Yuki Aoi^{a,1}, Hayao Hira^{b,1}, Yuya Hayakawa^c, Hongquan Liu^d, Kosuke Fukui^e, Xinhua Dai^d, Keita Tanaka^f, Ken-ichiro Hayashi^e, Yunde Zhao^d, Hiroyuki Kasahara^{g,h,*}

^aDepartment of Biological Production Science, United Graduate School of Agricultural Science, Tokyo University of Agriculture and Technology, Fuchu 183-8509, Japan ^bDepartment of Bioregulation and Biointeraction, Graduate School of Agriculture, Tokyo University of Agriculture and Technology, Fuchu 183-8509, Japan ^cDepartment of Applied Biological Science, Faculty of Agriculture, Tokyo University of Agriculture and Technology, Fuchu, Japan ^dSection of Cell and Developmental Biology, University of California San Diego, 9500 Gilman Drive, La Jolla, CA 92093-0116 ^eDepartment of Biochemistry, Okayama University of Science, Okayama, 700-0005, Japan ^fLaboratory of Biochemistry, Wageningen University & Research, 6708 WE Wageningen, the Netherlands ^gInstitute of Global Innovation Research, Tokyo University of Agriculture and Technology, Fuchu 183-8509, Japan ^hRIKEN Center for Sustainable Resource Science, Yokohama, Kanagawa 230-0045, Japan

Abstract

Auxin is a key plant growth regulator for diverse developmental processes in plants. Indole-3-acetic acid (IAA) is a primary plant auxin that regulates the formation of various organs. Plants also produce phenylacetic acid (PAA), another natural auxin, which occurs more abundantly than IAA in various plant species. Although it has been demonstrated that the two auxins have distinct transport characteristics, the metabolic pathways and physiological roles of PAA in plants remain unsolved. In this study, we investigated the role of Arabidopsis UDP-glucosyltransferase UGT84B1 in IAA and PAA metabolism. We demonstrated that UGT84B1, which converts IAA to IAA-glucoside (IAA-Glc), can also catalyze the conversion of PAA to PAA-glucoside (PAA-Glc), with a higher catalytic activity *in vitro*. Furthermore, we showed a significant increase in both the IAA and PAA levels in the *ugt84b1* null mutants. However, no obvious developmental phenotypes

*Corresponding author: kasahara@go.tuat.ac.jp.

¹These authors equally contributed to this work.

Author contributions

Y.A., H.H., and H.K. conceived and designed the research. Y.A. and H.H. performed most of the research. Y.A., H.H., Y.H., and K.T. carried out the enzyme assay and kinetic analysis of UGT84B1. K.F. and K.H. generated the transgenic plants. Y.Z. and H.L. generated the knockout mutants. K.H. synthesized the labeled compounds. Y.A. and H.K. analyzed the data. Y.A., Y.Z., and H.K. wrote the manuscript.

Accession numbers

UGT84B1: At2g23260.

Conflicts of interest

The authors have no conflicts of interest to declare.

Publisher's Disclaimer: This is a PDF file of an unedited manuscript that has been accepted for publication. As a service to our customers we are providing this early version of the manuscript. The manuscript will undergo copyediting, typesetting, and review of the resulting proof before it is published in its final form. Please note that during the production process errors may be discovered which could affect the content, and all legal disclaimers that apply to the journal pertain.

were observed in the *ugt84b1* mutants under laboratory growth conditions. Moreover, the overexpression of *UGT84B1* resulted in auxin-deficient root phenotypes and changes in the IAA and PAA levels. Our results indicate that UGT84B1 plays an important role in IAA and PAA homeostasis in Arabidopsis.

Keywords

auxin; indole-3-acetic acid; metabolism; phenylacetic acid; UDP-glucosyltransferase

1. Introduction

Auxin, a class of plant hormones, is essential for diverse developmental processes, including the formation of leaves, flowers, vasculature, adventitious roots, and lateral roots [1]. Plant organ development requires the formation of concentration gradients of indole-3-acetic acid (IAA), a primary natural auxin, in plant tissues. Endogenous IAA concentrations in plants are strictly regulated via multiple regulation steps: biosynthesis, inactivation, and polar auxin transport [2–4]. Previous studies concerning IAA inactivation in Arabidopsis revealed the occurrence of various auxin metabolic enzymes, such as GRETCHEN HAGEN 3 (GH3) auxin-amido synthetase, IAA CARBOXYL METHYLTRANSFERASE 1 (IAMT1), DIOXYGENASE FOR AUXIN OXIDATION (DAO), and the UDP-glucosyltransferase UGT84B1 (Fig. 1A) [5]. Members of the GH3 auxin-amido synthetases play important roles in the conversion of IAA to IAA-amino acid conjugates. For example, GH3.17/VAS2 forms IAA-glutamate (IAA-Glu) conjugate and plays an important role in hypocotyl elongation during the shade avoidance response [6]. IAMT1 catalyzes the conversion of IAA to IAA-methyl ester (MeIAA) and potentially regulates leaf development [7,8]. DAO-mediated oxidation of IAA to 2-oxindole-3-acetic acid (oxIAA) is essential for anther dehiscence, pollen fertility, and seed initiation in rice [9]. In Arabidopsis, oxIAA is further metabolized to oxIAA-glucoside (oxIAA-Glc) by UGT74D1 (Fig. 1A) [10]. IAA-glucoside (IAA-Glc) is one of the major IAA metabolites in angiosperms and gymnosperms [11–13]. Arabidopsis UGT84B1 catalyzes the glucosylation of IAA to IAA-Glc *in vitro* and *in vivo*, but its physiological role remains unclear [14,15]. The overexpression of *UGT84B1* causes a remarkable increase in IAA-Glc levels and severe auxin-deficient phenotypes in Arabidopsis [15]. Interestingly, *UGT84B1* overexpression also increases the levels of IAA [15], suggesting that certain hydrolases may actively hydrolyze IAA-Glc to IAA. UGT84B1 exhibits high catalytic activity towards IAA, but also uses various compounds, such as indole-3-butyric acid (IBA) and *cis*-cinnamic acid, as substrates *in vitro* [14]. These observations suggest that UGT84B1 may be implicated in the metabolism of various auxin-related compounds in Arabidopsis.

Phenylacetic acid (PAA), a natural auxin, regulates the expression of various auxin responsive genes via the TRANSPORT INHIBITOR RESPONSE 1/AUXIN SIGNALING F-BOX (TIR1/AFB) pathway [16,17]. IAA directionally moves and forms concentration gradients, whereas PAA does not show these polar transport characteristics in plants [16]. Based on this evidence, we recently proposed a model where IAA and PAA coordinately regulate plant growth and development [18]. In PAA metabolism, GH3s can catalyze the

conversion of PAA to its amino acid conjugates (Fig. 1B) [16,19]. More recently, we demonstrated that members of the GH3 family can modulate the ratio of IAA and PAA levels in Arabidopsis [20]. On the other hand, IAMT1 has been shown to exclusively metabolize IAA in Arabidopsis, despite it being able to convert both IAA and PAA to each carboxyl methyl ester *in vitro* [21]. A previous study on the role of UGT74B1 in glucosinolate biosynthesis demonstrated that it also catalyzes the glucosylation of PAA *in vitro* [22]. This suggests that UGT84B1 may play a crucial role in PAA metabolism in Arabidopsis.

In this study, we investigate the role of Arabidopsis UGT84B1 in the metabolism of IAA and PAA (Fig. 1A and B). We demonstrate that UGT84B1 expressed in *E. coli* can convert IAA to IAA-Glc and PAA to PAA-glucoside (PAA-Glc), with a higher catalytic activity towards PAA as a substrate. While no obvious developmental phenotypes were observed, the IAA and PAA levels significantly increased in the null *ugt84b1* mutants compared to those in the wild type (WT) plants, suggesting that UGT84B1 metabolizes both auxins in Arabidopsis. The overexpression of *UGT84B1* caused auxin-deficient phenotypes, but prompted a significant increase in the IAA and PAA levels. These results suggest that UGT84B1 metabolizes both IAA and PAA to the corresponding glucosides, while unidentified auxin-glucoside hydrolases revert these auxin metabolites back to active forms. Our results indicate that UGT84B1 plays a role in the regulation of IAA and PAA levels in Arabidopsis.

2. Materials and methods

2.1. Plant materials and growth conditions

The *Arabidopsis thaliana* ecotype Col-0 was used as the WT plants. Arabidopsis seeds were stratified at 4 °C for 2 days in the dark. Seedlings were grown on a Murashige and Skoog (MS) agar medium containing 1% sucrose at 23 °C under long-day light conditions with a 16 h light/8 h dark photoperiod. For β -estradiol (ER) treatment, *UGT84B1ox* and *pER8* plants [23] were grown vertically on an MS agar medium containing ER (2 μ M) for 7 days.

2.2. Chemicals

All chemicals were purchased from Sigma-Aldrich unless otherwise stated. [phenyl- $^{13}\text{C}_6$]IAA was purchased from Cambridge Isotope Laboratories. [phenyl- $^{13}\text{C}_6$]oxIAA, [$^{13}\text{C}_4$, ^{15}N]IAA-Asp, [$^{13}\text{C}_5$, ^{15}N]IAA-Glu, [phenyl- $^{13}\text{C}_6$]PAA, [$^{13}\text{C}_4$, ^{15}N]PAA-Asp, and [$^{13}\text{C}_5$, ^{15}N]PAA-Glu were previously synthesized [10,16,23]. IAA-Glc [1-*O*-(indol-3-ylacetyl)- β -D-glucose] and PAA-Glc [1-*O*-(2-phenylacetyl)- β -D-glucose] were synthesized according to the methods of Kai et al. [24]. Similarly, [2,2- D_2]IAA-Glc and [2,2- D_2]PAA-Glc were also synthesized as described in the supplementary data.

2.3. Preparation of recombinant UGT84B1 proteins

Total RNA was isolated from the WT plants using RNeasy (Qiagen, Venlo, Nether). The PrimeScriptTM RT reagent kit with gDNA eraser (Takara Bio, Kusatsu, Japan) was used to generate first-strand cDNA. The cDNA of the *UGT84B1* gene was cloned into a pCold-TF vector using the In-Fusion system (Takara Bio, Kusatsu, Japan). The *E. coli* strain BL21 star

(DE3) was transformed using the pCold-TF:UGT84B1 plasmid. The transformants were incubated at 37 °C in a TB medium with 50 µg/mL carbenicillin. Protein expression was induced by adding isopropyl β-D-1-thiogalactopyranoside at a final concentration of 0.2 mM. After incubation at 15 °C for 48 h, the cells were collected by centrifugation. The purification of the trigger factor (TF)-fused UGT84B1 proteins and removal of the TF tag by the Factor Xa were performed as previously described [21].

2.4. Biochemical and steady-state kinetic analysis of UGT84B1

As for the glucosyltransferase assay, IAA-Glc and PAA-Glc formation was analyzed using LC-MS/MS. In a 50 µL reaction, the standard assay conditions included a HEPES buffer (50 mM, pH 7.5), UDP-glucose (4 mM), MgSO₄ (2.5 mM), β-mercaptoethanol (14.2 mM), and IAA or PAA. The kinetic analysis of IAA and PAA used varied auxin concentrations (0, 10, 20, 30, 40, 80, and 150 µM). The enzyme reaction was initiated by the addition of the UGT84B1 protein (4 µg). The reactions were conducted at 30 °C for 2 hours. The reactions were terminated by adding 50 µL of acetonitrile containing [2,2-D₂]IAA-Glc or [2,2-D₂]PAA-Glc. The reaction mixtures were evaporated to dryness using a Speed Vac (Thermo Fisher Scientific, Waltham, MA). The samples were re-dissolved with 20 µL of H₂O and quickly injected into the LC-MS/MS system for IAA-Glc and PAA-Glc analysis. The HPLC separation and MS/MS analysis conditions are shown in Table S1. Steady-state kinetic parameters were calculated from a Lineweaver–Burk plot.

2.5. Generation of *ugt84b1* null mutants using CRISPR/Cas9 gene editing technology

A *UGT84B1* fragment (approximately 1.1 kb) was to be removed from the Arabidopsis genome using our CRISPR/Cas9 gene editing technology, which employs two gRNAs and cuts the target gene twice [25,26]. One target sequence was CCCGTGATCTCCTCTCCACCGT, and the other was GATTGGCGTTGGCACCTGGTGG (the underlined bold sequences were PAM sites). The knockout mutants were screened using a PCR-based methodology involving the UGT84B1-GT1 and UGT84B1-GT2 primers listed in Table S2. The PCR reaction should generate 0.75 and 1.9 kb bands for mutant and WT DNA, respectively. To further differentiate zygosity, a third primer (UGT84B1-GT3) was used (Table S2). The PCR reaction with primers UGT84B1-GT2 and UGT84B1-GT3 would produce a 0.5 kb band for both heterozygous and WT plants, but no band was produced for *ugt84b1* homozygous mutants. The two mutants used in this study had a deletion of 1159 and 1160 bp in UGT84B1, respectively.

2.6. Generation of *UGT84B1ox* plants

The full-length *UGT84B1* cDNA was obtained from the RIKEN BioResource Research Center, Japan. The *UGT84B1* ORF was amplified by adapter PCR from the RAFL cDNA clone using gene-specific (UGT84-F and UGT84-R) and adaptor attB primers (adaptor attB1 and attB2). The amplified *UGT84B1* fragment was cloned into the pDONR221 vector via the BP clonase II reaction and then transferred into the *pMDC7* vector [27] via the LR clonase II reaction (Invitrogen, Waltham, MA). Arabidopsis WT plants were transformed with the resulting construct, *pMDC7:UGT84B1*, using the floral dip method with the *Agrobacterium tumefaciens* GV3101 pMP90 strain.

2.7. qRT-PCR analysis

Total RNA was isolated from *pER8* and *UGT84B1ox* plants using RNeasy (Qiagen, Venlo, Nether). The PrimeScript™ RT reagent kit with a gDNA eraser (Takara Bio, Kusatsu, Japan) was used to generate first-strand cDNA. Quantitative RT-PCR (qPCR) was performed on a G8830A AriaMx Real-time PCR system (Agilent Technology, Santa Clara, CA) using a THUNDERBIRD SYBR qPCR mix (Toyobo, Osaka, Japan), for which the specific primers are listed in Table S2.

2.8. LC-MS/MS analysis of auxin metabolites

IAA, oxIAA, IAA-Asp, IAA-Glu, PAA, PAA-Asp, and PAA-Glu were analyzed as previously reported [18]. LC-ESI-MS/MS analysis of IAA-Glc was performed as described in the supplementary data.

3. Results

3.1. UGT84B1 catalyzes the conversion of PAA to PAA-Glc *in vitro*

To elucidate the glucosyltransferase activity of UGT84B1 against PAA, we expressed the TF-fused UGT84B1 proteins in *E. coli* using the pCold-TF vector. After the removal of the TF region, UGT84B1 proteins were reacted with IAA or PAA in the presence of UDP-glucose. We analyzed IAA-Glc and PAA-Glc using liquid chromatography-tandem mass spectrometry (LC-MS/MS). Authentic IAA-Glc was identified using a specific product ion at m/z 130.1, which was generated from a parent ion at m/z 336.0 (Fig. 1C). Similarly, authentic PAA-Glc was identified using a specific product ion at m/z 91.1, which was generated from a parent ion at m/z 297.1 (Fig. 1D). As shown in Fig. 1C, recombinant UGT84B1 proteins formed IAA-Glc from IAA and UDP-glucose, as previously described [14]. We found that UGT84B1 proteins also produced PAA-Glc from PAA and UDP-glucose (Fig. 1D). Assays in the absence of UGT84B1 proteins did not yield product ion peaks corresponding to IAA-Glc or PAA-Glc (Fig. 1C and D). Next, we performed a kinetics study on UGT84B1 with IAA and PAA as substrates. The determination of steady-state kinetic parameters for UGT84B1 highlighted the 6.4-fold higher catalytic efficiency (k_{cat}/K_m) for PAA than IAA (Table 1, Fig. S1). These results indicate that UGT84B1 may play a role in the metabolism of both IAA and PAA in Arabidopsis.

3.2. Both IAA and PAA levels increased in the *ugt84b1* knockout mutants

The physiological role of UGT84B1 in Arabidopsis has not yet been clarified, mainly due to the lack of analysis concerning its loss-of-function mutants. We generated CRISPR/Cas9-based knockout mutants of *ugt84b1* (*ugt84b1-c1* and *-c2*) [25], which are deletion mutants of 1159 and 1160 bp, respectively (Fig. 2A, Fig. S2). We found that our *ugt84b1-c1* and *-c2* lines did not exhibit obvious developmental phenotypes compared with WT plants under our normal laboratory growth conditions (Fig. S3). However, the IAA levels were significantly increased in *ugt84b1-c1* (1.3-fold) and *-c2* (1.4-fold) lines compared with those of WT plants (Fig. 2B). In addition, the IAA-Glc levels were decreased by 28% and 27% in *ugt84b1-c1* and *-c2* lines, respectively, implying that other auxin UGTs may also function in Arabidopsis. Moreover, the levels of oxIAA, IAA-aspartate (IAA-Asp), and IAA-Glu were

slightly increased in the *ugt84b1-c1* and *-c2* mutants compared with those of WT plants (Fig. 2B). These results suggest that a reduction in IAA glucosylation leads to an increase in IAA levels, which may promote other IAA inactivation pathways. Similar to IAA, the PAA levels were significantly increased by 1.2-fold in *ugt84b1-c1* and *-c2* mutants (Fig. 3C), suggesting that UGT84B1 also metabolizes PAA in Arabidopsis. These results suggest that UGT84B1 modulates the IAA and PAA levels in Arabidopsis through glucosylation.

We attempted to analyze the PAA-Glc levels in Arabidopsis plants, but were unable to quantify this metabolite using LC-MS/MS.

3.3. UGT84B1 overexpression alters the IAA and PAA levels in Arabidopsis

To further elucidate the role of UGT84B1 in IAA and PAA metabolism *in vivo*, we generated transgenic Arabidopsis plants that overexpress *UGT84B1* (*UGT84B1ox*) in an estradiol-inducible expression system using a pMDC7 vector. Two independent lines of *UGT84B1ox* (#10 and #31) displayed severe root growth defects compared to the empty-vector control *pER8* plants (Fig. 3A, 3B), which is consistent with the previously reported phenotypes of 35S promoter-driven *UGT84B1* overexpression plants [15]. Using quantitative RT-PCR (qPCR), we confirmed that the expression levels of *UGT84B1* were elevated by 5.5-fold in *UGT84B1ox* #10 lines (Fig. 3C), which displayed severe root growth defects compared with those in *pER8* plants. To investigate the impact of *UGT84B1* overexpression on auxin homeostasis, we quantified the levels of auxin metabolites in the roots of *pER8* and *UGT84B1ox* #10. Consistent with a previous study [15], the IAA-Glc levels were remarkably increased in *UGT84B1ox* (6.5-fold) (Fig. 3D). We also observed a significant increase in the IAA levels (12.7-fold) in *UGT84B1ox*, implying that accumulated IAA-Glc may be hydrolyzed to IAA by certain auxin-glucoside hydrolases. Moreover, the IAA-Asp and IAA-Glu levels were remarkably decreased in *UGT84B1ox*, suggesting the down-regulation of other IAA inactivation pathways for IAA homeostasis. Similar to IAA, we found that the PAA levels were increased by 1.9-fold in *UGT84B1ox* (Fig. 3D). Although the PAA-Glc levels in plants were not quantified, a significant increase in the PAA levels suggests that UGT84B1 also contributes to PAA metabolism *in vivo*.

4. Discussion

In this study, we provide evidence for the role that the auxin glucosyltransferase UGT84B1 plays in both IAA and PAA metabolism in Arabidopsis. First, we demonstrated that UGT84B1 proteins can catalyze the glucosylation of these auxins, with a higher substrate preference for PAA than IAA *in vitro*. Second, both IAA and PAA levels were significantly increased in Arabidopsis *ugt84b1* knockout mutants. Finally, the overexpression of *UGT84B1* caused the accumulation of both IAA and PAA in Arabidopsis, with remarkably increased IAA-Glc levels. Intriguingly, our CRISPR/Cas9-based knockout mutant of *ugt84b1-c1* did not show obvious developmental phenotypes (Fig. S3), even though the IAA and PAA levels were significantly increased (Fig. 2B). The reason that the *ugt84b1-c1* phenotype did not present the effects of increased auxin levels is unclear. However, we also found that *ugt84b1-c1* still produces large amounts of IAA-Glc (Fig. 2B), suggesting that other UGTs play a compensatory role in *ugt84b1-c1* mutants. As for the other Arabidopsis

IAA glucosyltransferases, UGT74E2, an IBA glucosyltransferase involved in the modulation of plant architecture and water stress response, exhibited a weak glucosyltransferase activity against IAA *in vitro* [11]. Moreover, UGT74D1, which mainly catalyzes the glucosylation of oxIAA to oxIAA-Glc, can form IAA-Glc *in vitro* [10,28]. Further analysis of multiple knockout mutants of UGT84B1 and these UGTs will help to elucidate the metabolic regulation of IAA in Arabidopsis.

Similar to IAA accumulation in 35S promotor-driven *UGT84B1* overexpression plants [15], a remarkable increase in the IAA levels was also observed in the estradiol-dependent *UGT84B1ox* plants, although the plants showed severe auxin-deficient root phenotypes (Fig. 3). Given that the IAA-Glc levels were remarkably increased in *UGT84B1ox* plants, these observations suggest that certain auxin-glucoside hydrolases play crucial roles in IAA-Glc homeostasis. Importantly, we observed an increase in the IAA (12.7-fold) and PAA levels (1.9-fold) in the *UGT84B1ox* plants compared to those in the *pER8* control plants (Fig. 3D). Since UGT84B1 exhibits glucosylation activity against both IAA and PAA *in vitro* (Table 1), the higher accumulation of IAA suggests that certain auxin-glucoside hydrolases may strongly favor IAA-Glc as a substrate in Arabidopsis. A previous study demonstrated that the *THOUSAND-GRAIN WEIGHT 6 (TGW6)* gene, which encodes IAA-Glc hydrolase, plays important roles in the regulation of grain length and weight in rice [29]. In contrast, auxin-glucoside hydrolases in Arabidopsis still remain unknown. As such, it is crucial to explore auxin-glucoside hydrolases in Arabidopsis to further understand the mechanisms of IAA and PAA homeostasis.

Supplementary Material

Refer to Web version on PubMed Central for supplementary material.

Acknowledgments

Funding

This study was supported by the Japan Society for the Promotion of Science (JSPS) KAKENHI [JP18H02457] to H.K. and [JP19H03253] to K.H. and H.K., and NIH (GM114660) to Y.Z.

Abbreviations:

IAA	indole-3-acetic acid
PAA	phenylacetic acid
IAA-Glc	IAA-glucoside
PAA-Glc	PAA-glucoside
LC-MS/MS	liquid chromatography-tandem mass spectrometry
gFW	gram fresh weight

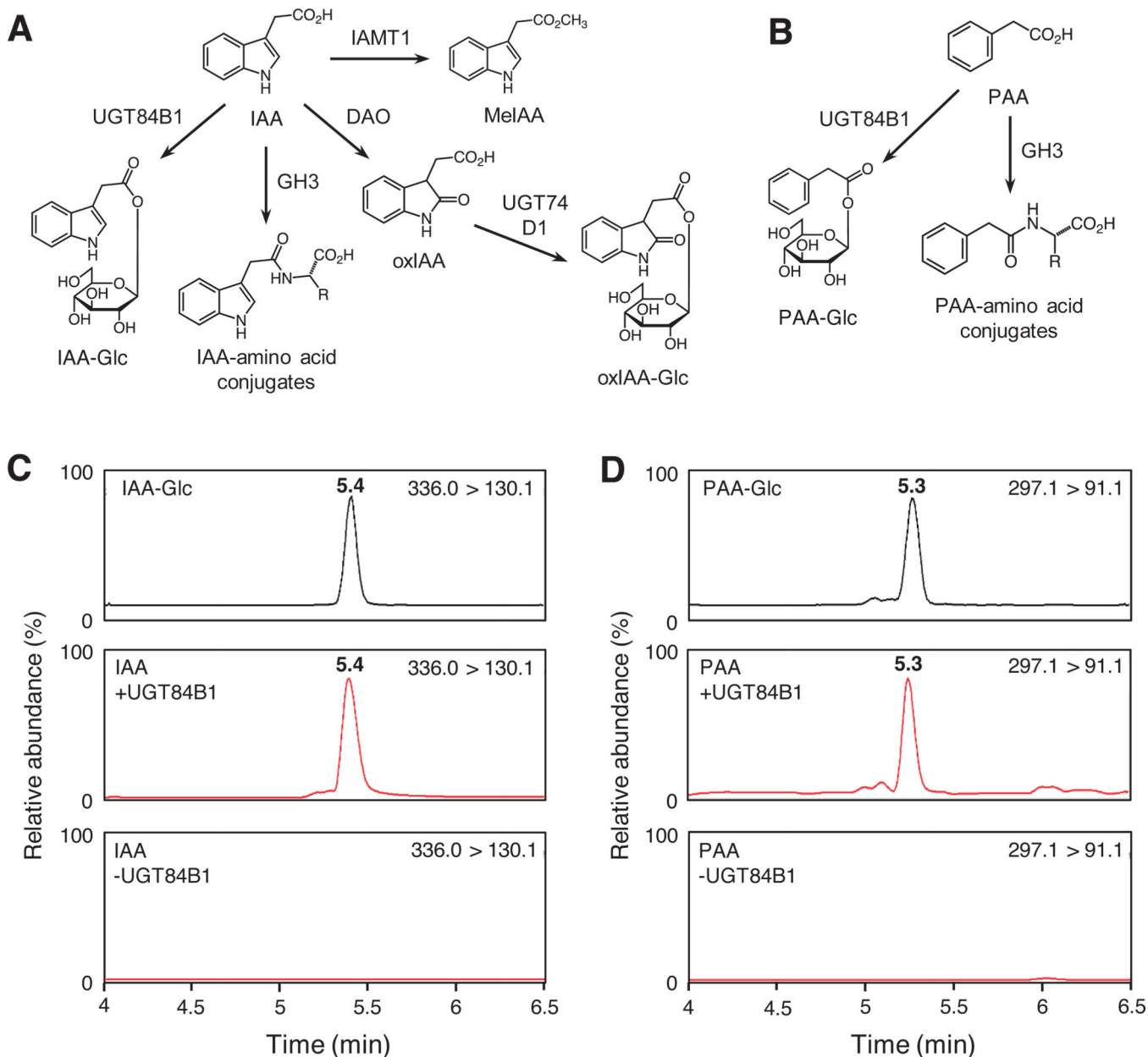
References

- [1]. Davies PJ, Plant hormones: Their Nature, Occurrence, and Functions, Springer, 2010, pp. 1–15. 10.1007/978-1-4020-2686-7.
- [2]. Kasahara H, Current aspects of auxin biosynthesis in plants, *Biosci. Biotechnol. Biochem.* 80 (2016) 34–42. 10.1080/09168451.2015.1086259. [PubMed: 26364770]
- [3]. Friml J, Subcellular trafficking of PIN auxin efflux carriers in auxin transport, *Eur. J. Cell Biol.* 89 (2010) 231–235. 10.1016/j.ejcb.2009.11.003. [PubMed: 19944476]
- [4]. Zhao Y, Auxin biosynthesis and its role in plant development, *Annu. Rev. Plant Biol.* 61 (2010) 49–64. 10.1146/annurev-arplant-042809-112308. [PubMed: 20192736]
- [5]. Korasick DA, Enders TA, Strader LC, Auxin biosynthesis and storage forms, *J. Exp. Bot.* 64 (2013) 2541–2555. 10.1093/jxb/ert080. [PubMed: 23580748]
- [6]. Zheng Z, Guo Y, Novák O, et al., Local auxin metabolism regulates environment-induced hypocotyl elongation, *Nat. Plants.* 2 (2016) 1–9. 10.1038/NPLANTS.2016.25.
- [7]. Qin G, Gu H, Zhao Y, et al., An indole-3-acetic acid carboxyl methyltransferase regulates Arabidopsis leaf development, *Plant Cell.* 17 (2005) 2693–2704. 10.1105/tpc.105.034959. [PubMed: 16169896]
- [8]. Qin Z, Lv H, Zhu X, et al., Ectopic expression of a wheat WRKY transcription factor gene TaWRKY71–1 results in hyponastic leaves in Arabidopsis thaliana, *PLoS One.* 8 (2013). 10.1371/journal.pone.0063033.
- [9]. Zhao Z, Zhang Y, Liu X, et al., A role for a dioxygenase in auxin metabolism and reproductive development in rice, *Dev. Cell.* 27 (2013) 113–122. 10.1016/j.devcel.2013.09.005. [PubMed: 24094741]
- [10]. Tanaka K, Hayashi KI, Natsume M, et al., UGT74D1 catalyzes the glucosylation of 2-oxindole-3-acetic acid in the auxin metabolic pathway in Arabidopsis, *Plant Cell Physiol.* 55 (2014) 218–228. 10.1093/pcp/pct173. [PubMed: 24285754]
- [11]. Tognetti VB, Van Aken O, Morreel K, et al., Perturbation of indole-3-butyric acid homeostasis by the UDP-glucosyltransferase UGT74E2 modulates Arabidopsis architecture and water stress tolerance, *Plant Cell.* 22 (2010) 2660–2679. 10.1105/tpc.109.071316. [PubMed: 20798329]
- [12]. Pên ík A, Casanova-Sáez R, Pila ová V, et al., Ultra-rapid auxin metabolite profiling for high-throughput mutant screening in Arabidopsis, *J. Exp. Bot.* 69 (2018) 2569–2579. 10.1093/jxb/ery084. [PubMed: 29514302]
- [13]. Brunoni F, Collani S, Casanova-Sáez R, et al., Conifers exhibit a characteristic inactivation of auxin to maintain tissue homeostasis, *New Phytol.* 226 (2020) 1753–1765. 10.1111/nph.16463. [PubMed: 32004385]
- [14]. Jackson RG, Lim EK, Li Y, et al., Identification and biochemical characterization of an Arabidopsis indole-3-acetic acid glucosyltransferase, *J. Biol. Chem.* 276 (2001) 4350–4356. 10.1074/jbc.M006185200. [PubMed: 11042207]
- [15]. Jackson RG, Kowalczyk M, Li Y, et al., Over-expression of an Arabidopsis gene encoding a glucosyltransferase of indole-3-acetic acid: Phenotypic characterisation of transgenic lines, *Plant J.* 32 (2002) 573–583. 10.1046/j.1365-313X.2002.01445.x. [PubMed: 12445128]
- [16]. Sugawara S, Mashiguchi K, Tanaka K, et al., Distinct characteristics of indole-3-acetic acid and phenylacetic acid, two common auxins in plants, *Plant Cell Physiol.* 56 (2015) 1641–1654. 10.1093/pcp/pev088. [PubMed: 26076971]
- [17]. Shimizu-Mitao Y, Kakimoto T, Auxin sensitivities of all Arabidopsis Aux/IAAs for degradation in the presence of every TIR1/AFB, *Plant Cell Physiol.* 55 (2014) 1450–1459. 10.1093/pcp/pcu077. [PubMed: 24880779]
- [18]. Mashiguchi K, Hisano H, Takeda-Kamiya N, et al., Agrobacterium tumefaciens enhances biosynthesis of two distinct auxins in the formation of crown galls, *Plant Cell Physiol.* 60 (2019) 29–37. 10.1093/pcp/pcy182. [PubMed: 30169882]
- [19]. Staswick PE, Serban B, Rowe M, et al., Characterization of an Arabidopsis enzyme family that conjugates amino acids to indole-3-acetic acid, *Plant Cell.* 17 (2005) 616–627. 10.1105/tpc.104.026690. [PubMed: 15659623]

- [20]. Aoi Y, Tanaka K, Cook SD, et al., GH3 auxin-amido synthetases alter the ratio of indole-3-acetic acid and phenylacetic acid in Arabidopsis, *Plant Cell Physiol.* 61 (2020) 596–605. 10.1093/pcp/pcz223. [PubMed: 31808940]
- [21]. Takubo E, Kobayashi M, Hirai S, et al., Role of Arabidopsis INDOLE-3-ACETIC ACID CARBOXYL METHYLTRANSFERASE 1 in auxin metabolism, *Biochem. Biophys. Res. Commun.* 527 (2020) 1033–1038. 10.1016/j.bbrc.2020.05.031. [PubMed: 32444138]
- [22]. Grubb CD, Zipp BJ, Ludwig-Müller J, et al., Arabidopsis glucosyltransferase UGT74B1 functions in glucosinolate biosynthesis and auxin homeostasis, *Plant J.* 40 (2004) 893–908. 10.1111/j.1365-313X.2004.02261.x. [PubMed: 15584955]
- [23]. Mashiguchi K, Tanaka K, Sakai T, et al., The main auxin biosynthesis pathway in Arabidopsis, *Proc. Natl. Acad. Sci. U. S. A.* 108 (2011) 18512–18517. 10.1073/pnas.1108434108. [PubMed: 22025724]
- [24]. Kai K, Nakamura S, Wakasa K, et al., Facile preparation of deuterium-labeled standards of indole-3-acetic acid (IAA) and its metabolites to quantitatively analyze the disposition of exogenous IAA in Arabidopsis thaliana, *Biosci. Biotechnol. Biochem.* 71 (2007) 1946–1954. 10.1271/bbb.70151. [PubMed: 17690468]
- [25]. Gao X, Chen J, Dai X, et al., An effective strategy for reliably isolating heritable and Cas9-free arabidopsis mutants generated by CRISPR/Cas9-mediated genome editing, *Plant Physiol.* 171 (2016) 1794–1800. 10.1104/pp.16.00663. [PubMed: 27208253]
- [26]. He Y, Zhao Y, Technological breakthroughs in generating transgene-free and genetically stable CRISPR-edited plants, *ABIOTECH.* 1 (2020) 88–96. 10.1007/s42994-019-00013-x.
- [27]. Curtis MD, Grossniklaus U, A gateway cloning vector set for high-throughput functional analysis of genes in planta, *Plant Physiol.* 133 (2003) 462–469. 10.1104/pp.103.027979. [PubMed: 14555774]
- [28]. Jin SH, Ma XM, Han P, et al., UGT74D1 is a novel auxin glycosyltransferase from Arabidopsis thaliana, *PLoS One.* 8 (2013) 1–11. 10.1371/journal.pone.0061705.
- [29]. Ishimaru K, Hirotsu N, Madoka Y, et al., Loss of function of the IAA-glucose hydrolase gene TGW6 enhances rice grain weight and increases yield, *Nat. Genet.* 45 (2013) 707–711. 10.1038/ng.2612. [PubMed: 23583977]

Highlights

- Arabidopsis UGT84B1 proteins catalyzed the glucosylation of both IAA and PAA *in vitro*.
- Both the IAA and PAA levels increased in the *ugt84b1* knockout mutants.
- The *ugt84b1* null mutants still produced IAA-glucoside.
- *UGT84B1* overexpression altered both the IAA and PAA levels in Arabidopsis.
- UGT84B1 homologs may also contribute to IAA and PAA homeostasis.

**Fig. 1.**

Enzyme activity of UGT84B1 proteins with IAA and PAA

(A) Schematic representation of the IAA metabolic pathways in plants. (B) Schematic representation of the PAA metabolic pathways in plants. (C) MS/MS chromatogram (m/z 336.0 > 130.1) of authentic IAA-Glc (upper), the reaction product of UGT84B1 with IAA (middle), and the control without UGT84B1 (lower). IAA-Glc is detected at 5.4 min. (D) The MS/MS chromatogram (m/z 297.1 > 91.1) of authentic PAA-Glc (upper), the reaction product of UGT84B1 with PAA (middle), and the control without UGT84B1 (lower). PAA-Glc is detected at 5.3 min.

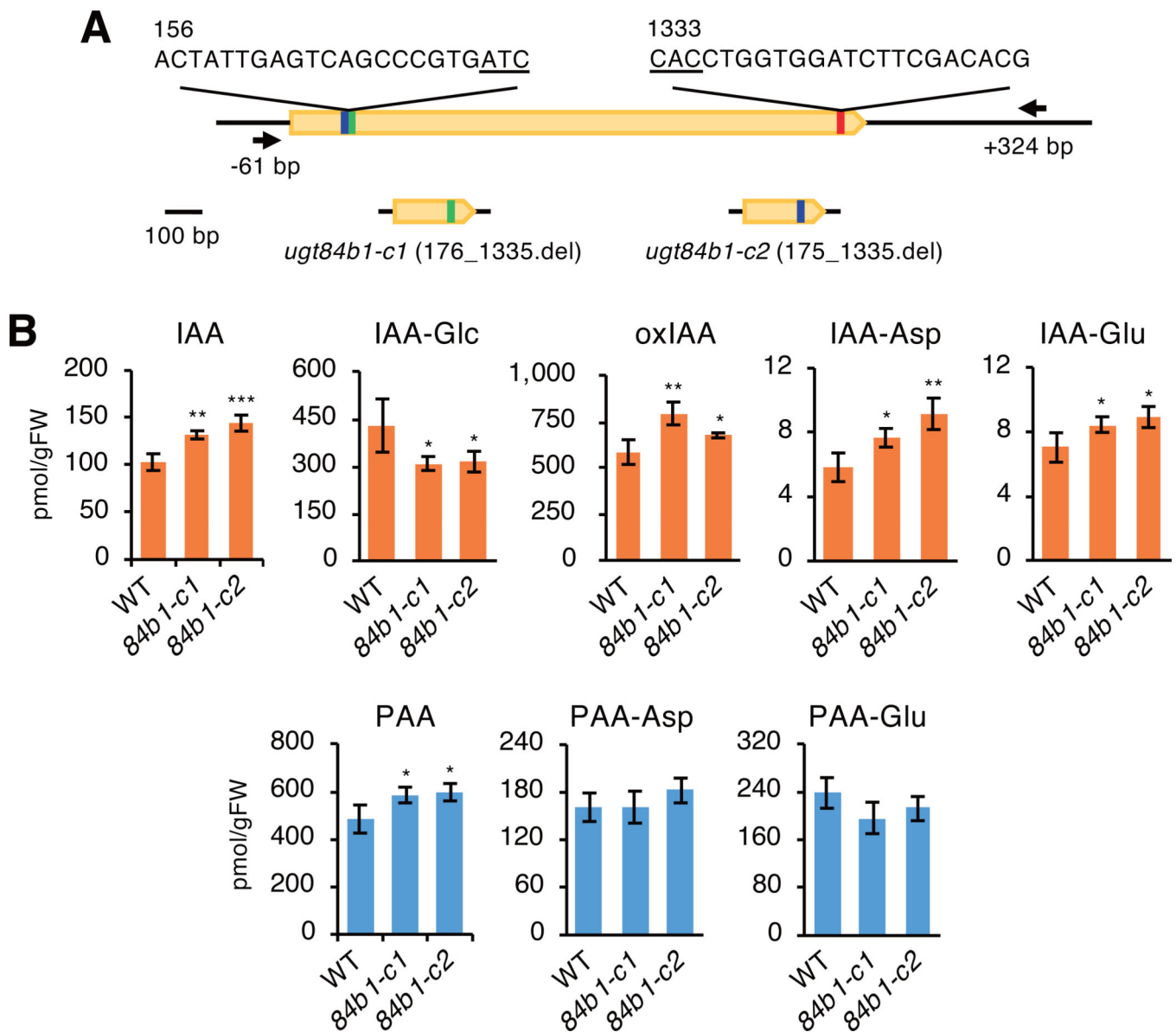
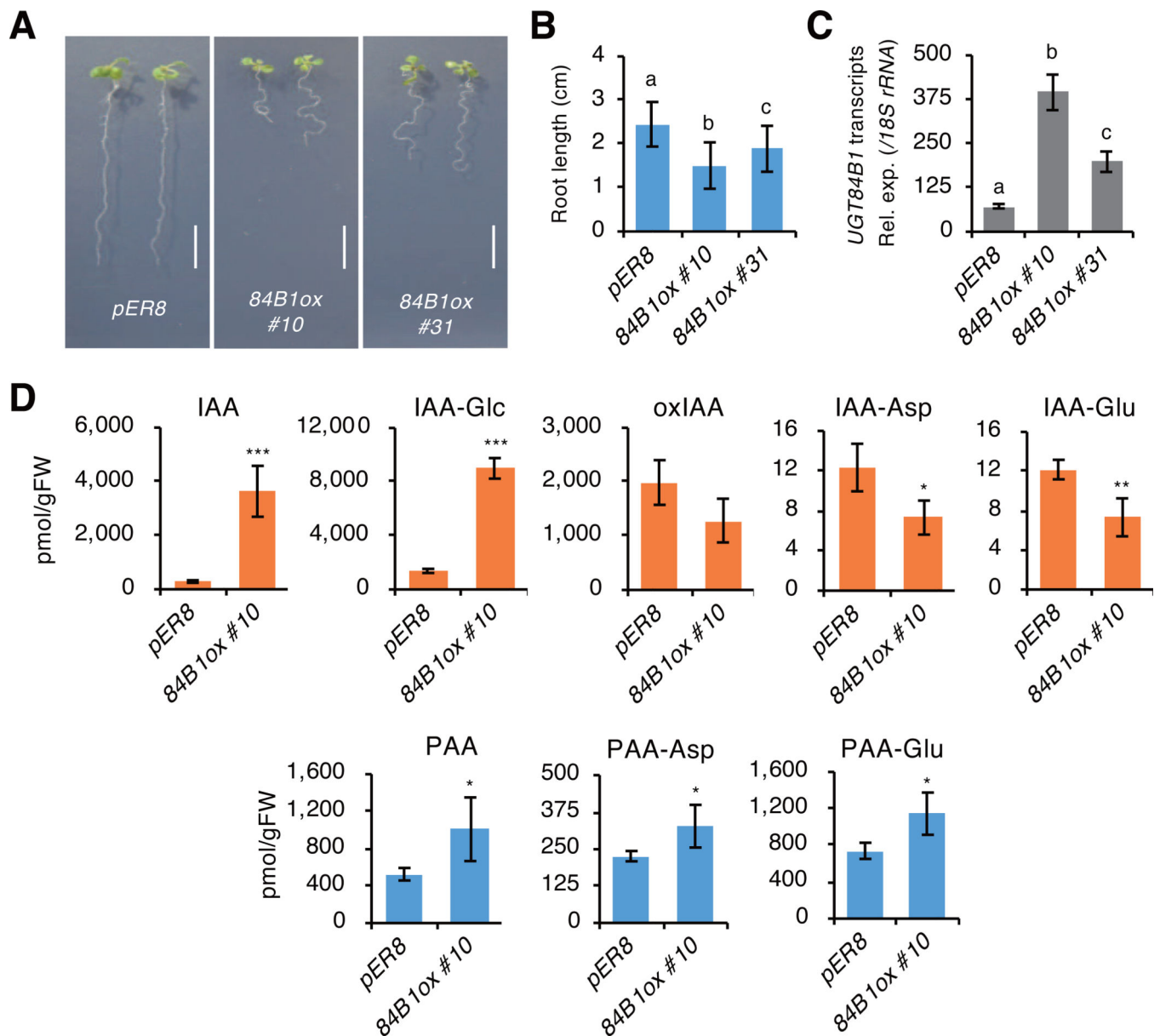


Fig. 2.

Characterization of *ugt84b1* knockout mutants

(A) Mutations in *ugt84b1-c1* and *-c2* mutants. Orange box represents the exon in the *UGT84B1* gene. Underlines indicate PAM sites. Arrows indicate the gene-specific primers used for genotyping. (B) The levels of IAA and PAA metabolites in 10-day-old *ugt84b1-c1* (*84b1-c1*) and *-c2* (*84b1-c2*) mutants. Values are the means \pm SD ($n = 4$). Differences between the WT plants and *84b1-c1/-c2* mutants are statistically significant at $P < 0.05$ (* $P < 0.05$, ** $P < 0.01$, and *** $P < 0.001$, Student's *t*-test).

**Fig. 3.**

Analysis of *UGT84B1ox* plants

(A) Phenotypes of *pER8* and *UGT84B1ox* (*84B1ox*) seedlings treated with ER (2 μ M) for 7 days. Scale bars indicate 1 cm. (B) Primary root length of *pER8* and *84B1ox* seedlings treated with ER for 7 days. Values are the means \pm SD ($n = 35$). (C) Expression levels of *UGT84B1* in *pER8* and *84B1ox* seedlings treated with ER for 7 days. Differences between *pER8* and *84B1ox* plants are statically significant at $P < 0.01$ (ANOVA, Tukey test). (D) The levels of IAA and PAA metabolites in *pER8* and *84B1ox* plants. Plants (6 days old) were treated with ER for 4 days. Values are the means \pm SD ($n = 4$). Differences between *pER8* and *84B1ox* plants are statistically significant at $P < 0.05$ (* $P < 0.05$, ** $P < 0.01$, and *** $P < 0.001$, Student's *t*-test).

Table 1.

Kinetic analysis of UGT84B1 proteins with IAA and PAA

Steady-state kinetic parameters were determined for IAA and PAA as described in the Materials and Methods.

The average values \pm SD ($n = 3$) are shown.

Substrate	K_m (μM)	V_{max} ($\mu\text{M min}^{-1}$)	k_{cat} (min^{-1})	k_{cat}/K_m ($\text{mM}^{-1} \text{s}^{-1}$)
IAA	23.07 ± 3.64	0.16 ± 0.01	0.1 ± 0.01	0.07 ± 0.01
PAA	32.34 ± 2.64	1.46 ± 0.09	0.88 ± 0.05	0.45 ± 0.01

Author Manuscript

Author Manuscript

Author Manuscript

Author Manuscript